American Mineralogist, Volume 83, pages 1316–1322, 1998

Octahedral site Fe^{2+} quadrupole splitting distributions from the Mössbauer spectra of arrojadite

ISAMU SHINNO[1,*] AND ZHE LI[2]

[1]Graduate School of Social and Cultural Study, Kyushu University, Fukuoka 810, Japan
[2]Institute of Geology, Chinese Academy of Science, Beijing 100029, China

ABSTRACT

The Mössbauer spectra of arrojadite, $(K,Ba)(Na,Ca)_5(Fe^{2+},Mn,Mg)_{14}Al(PO_4)_{12}(OH,F)$, at 298 and 95 K were investigated for the first time. The spectra at both temperatures were analyzed in terms of their Fe^{2+} quadrupole splitting distributions (QSDs). The overall QSDs at both temperatures can be interpreted in terms of five octahedral site Fe^{2+} QSD contributions. The quadratic elongation, $\langle\lambda\rangle$, and the variation of bond angles, σ^2, for the different sites were calculated on the basis of the structural data obtained by Moore et al. (1981). The five QSD contributions are tentatively assigned to Fe^{2+} in the M3, M4, M5, M6, and M7 sites, based on the structural determination and the relation of the quadrupole splitting to the distortion of the octahedra, respectively. The Fe^{2+} ions are randomly distributed over the M3, M4, M5, M6, and M7 sites. In addition, Mössbauer data from arrojadite and related phosphate minerals indicate that the mean value of the isomer shift of Fe^{2+} in the octahedral sites in phosphate minerals is ~0.07 mm/s larger than that in silicate minerals. This difference is explained in terms of electron affinity.

INTRODUCTION

To date, many Mössbauer spectra of silicate and oxide minerals have been published, but relatively few Mössbauer studies concern phosphate minerals. Gonser and Grant (1967) first examined single and polycrystalline samples of naturally occurring vivianite, $Fe_3(PO_4)_2 \cdot 8H_2O$; subsequently, the oxidation mechanism of vivianite has been investigated many times (Takashima and Ohashi 1968; Tricker and Ash 1979; Vochten et al. 1979; Dormann and Poullen 1980; McCammon and Burns 1980; Burns 1981). Chandra and Hoy (1967) reported that the ordered phase of ludlamite, $Fe_3(PO_4)_2 \cdot 4H_2O$, has a Mössbauer spectrum with two hyperfine fields below 15 K. Lithium orthophosphate, $LiFe_{0.8}Mn_{0.2}PO_4$, orders antiferromagnetically at low temperature (Schideler and Terry 1969). Kostiner (1972) reported the Mössbauer parameters for the phosphate minerals triplite, zwieselite, triploidite, and wolfeite. The cation distributions of the ternary orthophosphates, $(Zn, Fe, Me)_3(PO_4)_2$, (Me = Ni, Mg, Co), and $(Co, Fe)_3(PO_4)_2$, having the farringtonite structure were investigated by Nord and Ericsson (1985) and Nord et al. (1985). The cation partitioning in hydrothermally prepared sarcopsites $(Fe,Mn,Co,Mg)_3(PO_4)_2$ was analyzed by means of X-ray powder diffraction and ^{57}Fe Mössbauer spectroscopy (Ericsson et al. 1986; Charalampides et al. 1988). All of the above studies provide useful information on the crystal chemistry and bonding in phosphate minerals.

The arrojadite-dickinsonite family constitutes an alkali transition metal phosphate group. Several mineralogical studies on arrojadite-dickinsonite were carried out (Headden 1891; Ziegler 1914; Quensel 1937; Mason 1941; Guimaraes 1942; Lindberg 1950). Moore and Ito (1979) analyzed 12 samples of the family and proposed the general formula $XY_5M^{2+}_{14}Al(PO_4)_{12}(OH,F)$, where X = large cations such as K^{1+}, Ba^{2+}, Y = (Na^{1+}, Ca^{2+}) and M = $(Fe^{2+}, Mn^{2+}$ and $Mg^{2+})$. Moore et al. (1981) determined the crystal structure for the series using single-crystal X-ray diffraction. In this study, intrinsic Fe^{2+} QSDs were extracted from Mössbauer spectra of arrojadite at 298 and 95 K, and the iron distributions over the different sites are determined.

EXPERIMENTAL METHODS

The sample occurs as large cleavable masses in a granitic pegmatite from India associated with feldspar, quartz, muscovite, beryl, and spodumene. The purity of the arrojadite was checked using X-ray diffraction and no other phases were found. Its chemical composition was analyzed using a Cameca SX51 electron microprobe. The analyses were carried out on six arrojadite crystals with colors ranging from olive to grass green. The average composition is Na_2O 6.83 (6.13–7.85), K_2O 1.84 (1.70–1.88), CaO 2.59 (2.43–2.68), MnO 14.76 (14.16–15.50), FeO 28.33 (27.60–28.79), MgO 1.18 (1.01–1.24), Al_2O_3 2.45 (2.35–2.51), P_2O_5 41.71 (40.32–43.10), total 99.69 wt% (97.05–102.28), where the brackets denote the ranges. The chemical formula can be written as $K_{0.81}(Na_{4.60}Ca_{0.95})_{5.55}(Mn_{4.34}Fe_{8.23}Mg_{0.61})_{13.18}Al_{1.00}(P_{12.25}O_{48})(OH,F)$, based on 48 O atoms in the formula unit.

* E-mail: Shinno@rc.kyushu-u.ac.jp

0003–004X/98/1112–1316$05.00

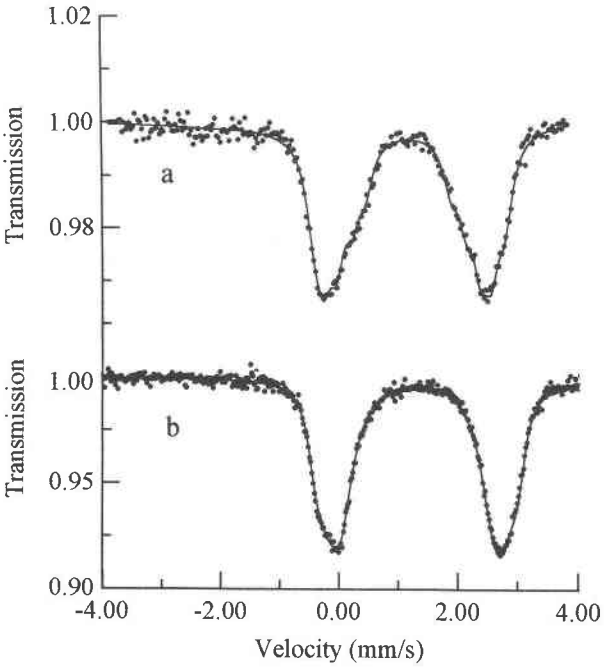

FIGURE 1. Mössbauer spectra of arrojadite at 298 K (**a**) and 95 K (**b**). Dots are the data. Solid line = the fit for one generalized site with five QSD Gaussian components.

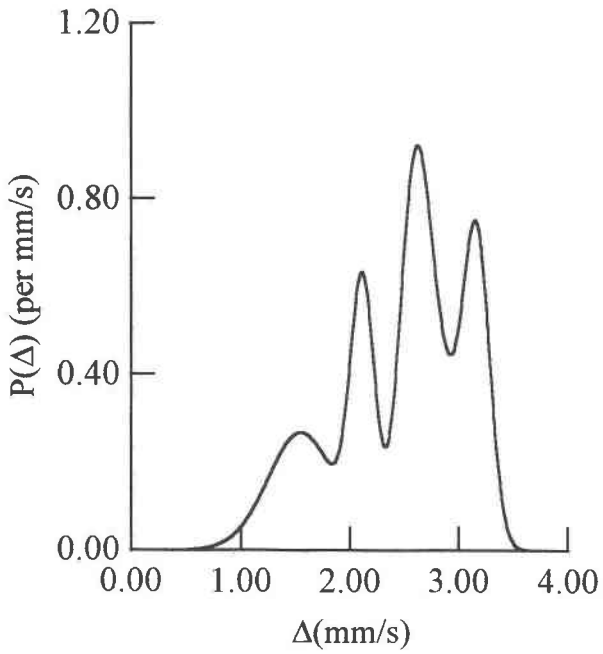

FIGURE 2. The octahedral-site Fe^{2+} QSDs of arrojadite at 298 K.

The Mössbauer spectrum of arrojadite was measured at 298 K using a computer-controlled constant acceleration Mössbauer spectrometer (PH-805) with 512 channels, whereas the spectrum at 95 K was obtained with a constant acceleration spectrometer (Austin Science Associates) in conjunction with a 1024 multichannel analyzer (ORTEC MCA 7700) and an OXFORD 41074 instrument cryostat with a temperature range of 77–300 K and a variation of 0.1 K. An approximately 5 mCurie ^{57}Co source in a palladium matrix was used in the measurements. The detector used is a xenon (methane) proportional counter. The velocity scales were normalized with respect to the center of the spectrum of metallic iron foil at 298 K.

A Voigt-based method for arbitrary shape QSDs and hyperfine field distributions (HFDs) has been developed (Rancourt and Ping 1991a, 1991b; Ping et al. 1991; Rancourt 1994a, 1994b; Rancourt et al. 1994; Rancourt et al. 1996). This method was used to fit the raw spectra in this study. The method assumes a certain number m of generalized sites each having their own continuous QSD. Each normalized site-specific QSD is composed of a certain number (n_i for site i) of Gaussian components being the sum of more than one Voigt line. The corresponding fit can be expressed as $n_1 - n_2 - \ldots - n_m$ V. The center shift δ of each site's distribution component is related to its quadrupole splitting, Δ, as $\delta = \delta_0 + \delta_1\Delta$, where δ_0 is the value of δ when the distributed hyperfine parameter has a value of zero, and δ_1 is the coupling of δ to the distributed hyperfine parameter. Therefore, at most $2 + 2m + 3\sum_{i=1}^{m} n_i$ fitting parameters are required: two spectrum-specific parameters (BG, background, Γ, half width), two site-specific parameters (δ_0, δ_1), and three component-specific parameters (h, the height of one line in the symmetric elemental Lorentzian doublet; Δ, the center of the Gaussian QSD component; σ_Δ, the width of the Gaussian QSD component).

The Voigt-based QSD method is used to describe the intrinsic Mössbauer line shape (the thin-limit spectrum). In this case, the only correct Lorentzian line width, Γ, is the natural one, i.e., $\Gamma = 0.194$ mm/s. Because finite absorber thickness can cause spectral broadening, the raw spectra should be corrected for thickness before the Voigt-based QSD method is used. Ping et al. (1991) investigated quasi-crystals by using the Voigt-based method, with the absorber thicknesses in the range of 0.005–0.087 mg $^{57}Fe/cm^2$. In their study, the full thickness correction was not performed and the Γ obtained is in the range of 0.214–0.279 mm/s. In this study, the absorber thickness is small, 0.006 mg $^{57}Fe/cm^2$, and hence the Voigt-based method was used directly. The resulting Γ values equal 0.279 mm/s at 298 K and 0.289 mm/s at 95 K, respectively.

RESULTS

The Mössbauer spectra of arrojadite at 298 and 95 K each consists of two broad peaks, and the spectrum at 298 K shows very small shoulders, indicating ferrous ions in several crystallographic sites in the crystal structure (Fig. 1). The octahedral-site Fe^{2+} QSDs obtained from fitting the spectra are shown in Figures 2 and 3. The calculated Mössbauer parameters for the QSDs are summarized in Table 1.

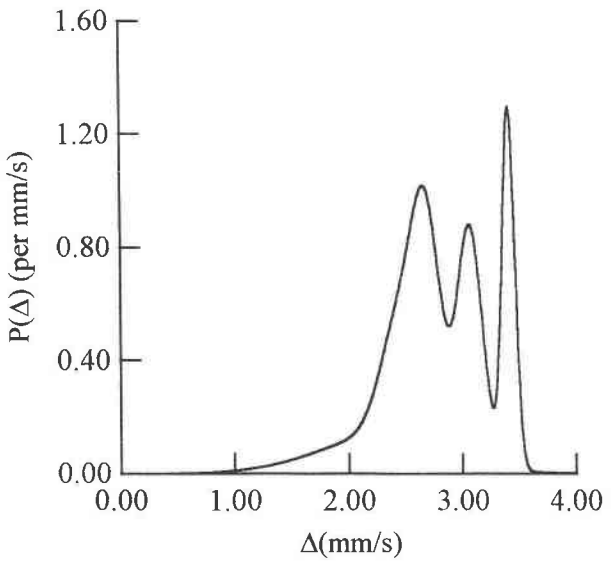

FIGURE 3. The octahedral-site Fe^{2+} QSDs of arrojadite at 95 K.

DISCUSSION

Interpretation of Fe^{2+} quadrupole splitting distributions

From single-crystal X-ray diffraction techniques (Moore et al. 1981) arrojadite is monoclinic, a = 16.45 Å, b = 10.03 Å, c = 25.70 Å, and β = 112.33°, with space group $C2/c$ and Z = 4. Forty-nine nonequivalent atoms occur in the asymmetric unit cell. There are 15 crystallographically distinct cations and 6 distinct PO_4 tetrahedra. Seven of the 15 cations in the M sites contain transition metal cations such as Fe^{2+}. The M1 site is a distorted tetrahedron, M2 is a distorted square pyramid, M7 is either a square pyramid or an octahedron, with O(4x) included as a coordinating anion, and M3, M4, M5, and M6 are distorted octahedra. The Al atom is located in a distorted octahedral site. Large cation sites are labeled X. X1 is a site half-occupied by Ca^{2+}. The sites X2, X3, and X6 are predominately occupied by Na^{1+}, and X4, X5, and X7 are occupied by either K^{1+} or Na^{1+}.

Mössbauer spectroscopy is sensitive to the local chemical and crystallographic environment. Each distinct chemical and crystallographic environment for Fe forms one pair of Lorentzian lines in the Mössbauer spectrum. This model has been successfully used to interpret most Mössbauer spectra of minerals. However, when tetrahedral and octahedrally coordinated sites accommodate a large variety of cations, minerals often display a wide range of local environments. This leads to a continuous distribution of quadrupole splitting. In this case, the QSD method should be used to analyze Mössbauer spectra. Arrojadite falls in the later case consisting of two broad peaks. Probably, several QSDs may be contained in the Mössbauer spectra of arrojadite.

To date, a synthetic annite-oxyannite series and synthetic and natural Al-deficient members of the phlogopite-annite series have been analyzed by QSDs method (Rancourt 1994a, 1994b; Rancourt et al. 1994; Rancourt et al. 1996). There are cis and trans octahedra occupied by cations in mica structure. According to Fe^{2+} QSDs analysis of synthetic annites, the overall QSDs can be interpreted in terms of four QSD contributions centered at $\Delta \sim 2.55$ mm/s for $Fe^{2+}O_4(OH)_2$ octahedra (cis and trans not resolved), $\Delta \sim 2.35$ mm/s for $Fe^{2+}O_4(OH)F$ octahedra (cis and trans not resolved), $\Delta \sim 2.15$ mm/s for cis-$Fe^{2+}O_4F_2$ octahedra, and $\Delta \sim 1.5$ mm/s for trans-$Fe^{2+}O_4F_2$ octahedra (Rancourt 1996). Thus, the QSD method can provide information about local distortion and chemical environments.

We tried to fit the spectra of arrojadite at 298 and 95 K to m = 1 generalized sites with n_1 = 1 to 8 and m = 5 with n_5 = 1. The fits with m = 5 (n_5 = 1) are divergent, but the fits with m = 1 (n_1 = 1, 2, 3, 4, 5, 6, 7, or 8) are convergent. Because the broad doublet spectrum is not well resolved, several different models with m = 1 (n_1 = 1, 2, 3, 4, 5, 6, 7, 8) could be fit that are convergent. Because χ_r^2 for the model with m = 1 (n_1 = 5) is smaller than those for the models with m = 1 (n_1 = 1, 2, 3, or 4), and some of the values Δ_σ for the models with m = 1 (n_1 = 6, 7, or 8) are too small, the model with m = 1 (n_1 = 5) is preferred. Many different initial values of the Mössbauer parameters for this model were used to try to fit the spectra. Table 1 lists the fit with the smallest χ_r^2 values. This model may not be unique, but it is consistent with the crystal structure of arrojadite, discussed below.

Table 2 summarizes the Mössbauer parameters at 298 K for other phosphate minerals. The isomer shifts of Fe^{2+} in octahedral and distorted bipyramidal coordination lie

TABLE 1. Mössbauer parameters for arrojadite

T (K)	δ_0 (mm/s)	δ_1	δ (mm/s)	Δ (mm/s)	σ_Δ (mm/s)	Area (%)	Γ (mm/s)	Assignment	χ_r^2
298			1.271	3.171	0.107	22		Fe^{2+}(M3)	
			1.268	2.765	0.149	22		Fe^{2+}(M6)	
	1.246	0.008	1.266	2.513	0.181	24	0.279	Fe^{2+}(M7)	1.27
			1.263	2.071	0.097	14		Fe^{2+}(M4)	
			1.258	1.524	0.267	18		Fe^{2+}(M5)	
95			1.313	3.414	0.054	19		Fe^{2+}(M3)	
			1.315	3.071	0.111	23		Fe^{2+}(M6)	
	1.332	−0.006	1.317	2.692	0.122	21	0.289	Fe^{2+}(M7)	1.04
			1.318	2.478	0.182	20		Fe^{2+}(M4)	
			1.319	2.251	0.552	17		Fe^{2+}(M5)	

Note: The last decimal place is uncertain.

TABLE 2. Mössbauer parameters for some phosphate minerals

Mineral and formula	δ (mm/s)*	Δ (mm/s)	Assignment	*d*(Å)‡	References
Vivianite	1.15	2.51	Fe^{2+}(I)	2.007	Mattievich and Danon (1977)§
$Fe_3(PO_4)_2(H_2O)_4$	1.20	2.97	Fe^{2+}(II)	2.017	Mori and Ito (1950)‖
Ludlamite	1.18	2.41	Fe^{2+}(I,II)	2.116	Mattievich and Danon (1977)§
$Fe_3(PO_4)_2(H_2O)_4$					Ito and Mori (1951)‖
Phosphoferrite	1.18	2.37	Fe^{2+}(I)	2.160	Mattievich and Danon (1977)§
$Fe_3(PO_4)_2(H_2O)_3$	1.19	1.55	Fe^{2+}(II)	2.170	Moore and Akari (1976)‖
Hureaulite	1.26	2.47	Fe^{2+}(II)	2.159	Nomura and Ujihira (1982)§
$(Mn_{0.83}Fe_{0.17})H_2(PO_4)_4(H_2O)_4$	1.26	1.48	Fe^{2+}(I)	2.188	Moore and Araki (1973)‖
	1.23	1.20	Fe^{2+}(III)	2.209	
Sarcopsite	1.22	2.88	Fe^{2+}(M1,M2)	2.17	Ericsson and Nord (1984)§‖
$(Fe_{0.8}Mn_{0.2})_3(PO_4)_2$					
Sarcopsite	1.21	2.99	Fe^{2+}(M1,M2)	2.13	Ericsson and Nord (1984)§
$(Ni_{0.3}Fe_{0.7})_3(PO_4)_2$					Moore (1972)‖
Farringtonite	1.12	2.86	Fe^{2+}(M1)†	2.06	Nord and Ericsson (1985)§‖
γ-$(Zn_{0.7}Fe_{0.2}Ni_{0.1})_3(PO_4)_2$	1.27	1.78	Fe^{2+}(M2)	2.13	
Farringtonite-related phase	1.12	2.78	Fe^{2+}(M1)†	2.02	Nord et al. (1985)§‖
γ-$CO_2Fe(PO_4)_2$	1.27	0.93	Fe^{2+}(M2)	2.15	
Graftonite	1.19	2.10	Fe^{2+}(M1)	2.231	Nord and Ericsson (1982)§‖
$Fe_3(PO_4)_2$	1.11	1.59	Fe^{2+}(M2)†	2.134	
	1.16	2.37	Fe^{2+}(M3)†	2.104	
Graftonite-related phase	1.20	2.05	Fe^{2+}(M1)	2.37	
$(Fe_{0.5}Mn_{0.5})_3(PO_4)_2$	1.10	1.57	Fe^{2+}(M2)†	2.00	Nord and Ericsson (1982)§‖
	1.16	2.38	Fe^{2+}(M3)†	2.03	
Triplite	1.227	2.700	Fe^{2+}(M1)	2.202	Kostiner (1972)§
$(Mn_{0.95}Fe_{0.25}Mg_{0.70}Ca_{0.10})PO_4F$	1.274	2.010	Fe^{2+}(M2)	2.153	Waldrop (1969)‖
Triploidite	1.190	2.148	Fe^{2+}(M1,4,6,8)	2.126	Kostiner (1972)§
$(Mn,Fe)_2PO_4OH$	1.198	1.776	Fe^{2+}(M2,3,5,7)	2.205	Waldrop (1970)‖

Notes: * δ (mm/s) are relative to α-Fe.
† (M1), (M2), and (M3) are distorted bipyramid, and the rest of sites are octahedra.
‡ The mean bond length.
§ Mössbauer parameters were reported.
‖ Bond lengths were reported.

in the range of 1.15–1.27 mm/s and 1.10–1.16 mm/s, respectively. As discussed below, the isomer shifts are related to the coordination numbers and average bond lengths. The values of the isomer shift increase with increase in coordination number and average bond length (Fig. 4). The isomer shift at 298 K for arrojadite studied here is in the range of 1.26 ± 0.01 mm/s, indicating that the Fe^{2+} cations are distributed over the octahedral sites M3–M7 rather than the distorted square pyramid M2 site.

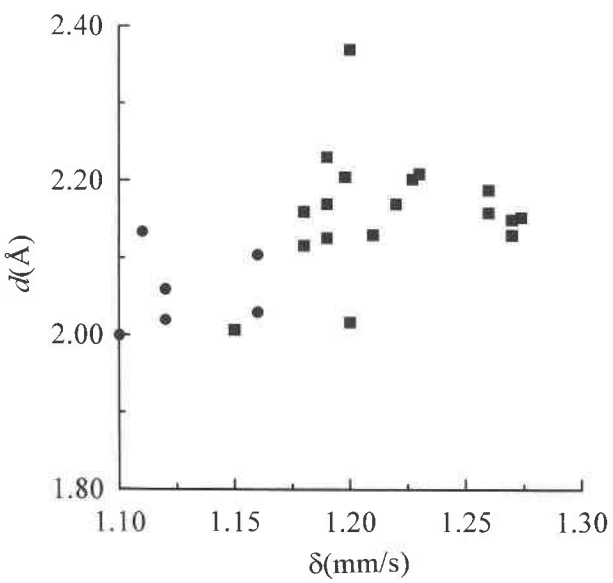

FIGURE 4. The correlation of bond length with isomer shift for phosphate minerals of Table 2. The solid circles and squares denote bipyramids and octahedral sites, respectively.

Ingalls (1964) proposed that the quadrupole splitting for ferrous iron in near octahedral coordination could be described as follows:

$$\Delta = \Delta\,(0)\ \alpha^2\ F(\Delta_1, \Delta_2, \lambda_0, \alpha^2, T) \qquad (1)$$

where Δ(0) is the maximum possible value of the quadrupole splitting, F the reduction function, whose value is given by perturbation theory, Δ_1 and Δ_2 the two lowest splittings of the crystal-field levels, α^2 a covalence factor, λ_0 a spin-orbit coupling constant, and T the absolute temperature. In general, the values of Δ_1 and Δ_2 can be used to express the distortion of the polyhedron. Ingalls (1964) demonstrated that the quadrupole splitting increases very rapidly with increasing octahedral distortion at small distortions, then after reaching a maximum, it decreases slowly with further distortion.

Various crystallographic criteria have been proposed to describe the distortions of coordination polyhedra from their holosymmetric geometries. Quadratic elongation, $\langle\lambda\rangle$, and variance of bond angles, σ^2, were used to describe octahedral distortion by Robinson et al. (1971):

$$\langle\lambda\rangle = \sum_{i}^{6} (l_i/l_0)^2/6 \qquad (2)$$

$$\sigma^2 = \sum_{i=1}^{12} (\theta_i - 90)^2/11 \qquad (3)$$

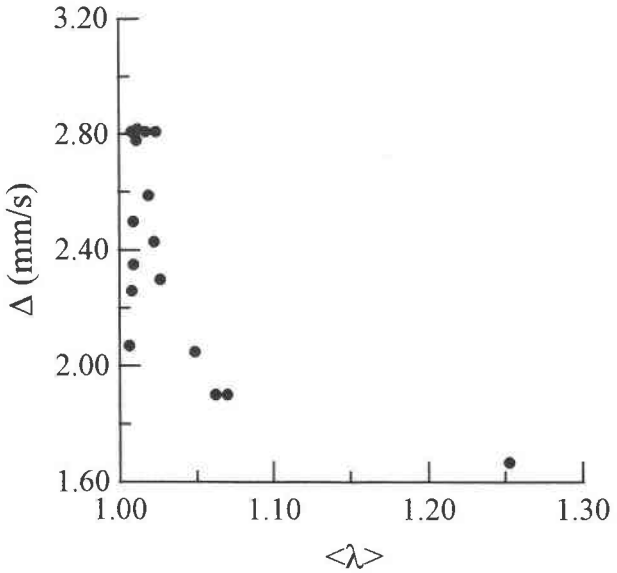

FIGURE 5. The correlation of the quadrupole splitting to the quadratic elongation in chain silicates (Li and De Grave, in preparation).

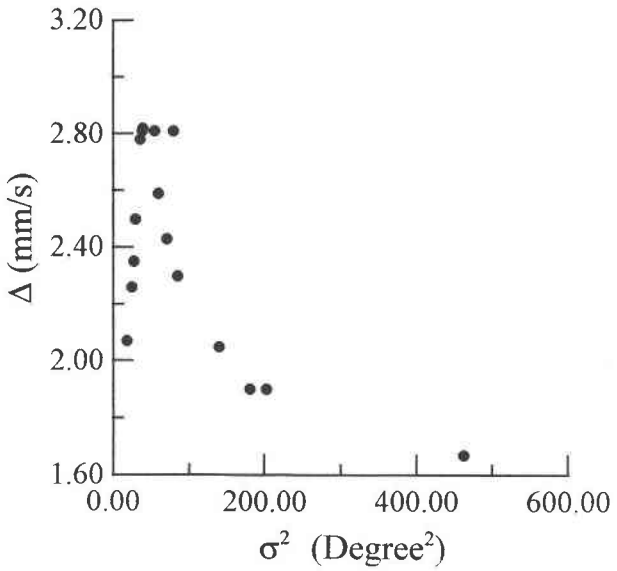

FIGURE 6. The correlation of the quadrupole splitting to the variance of bond angles in chain silicates (Li and De Grave, in preparation).

where l_0 is distance from the center to vertex for an octahedron with O_h symmetry, whose value is equal to that of a distorted octahedron with bond length l_i, and θ_i represents the angles between the metal-oxygen bonds. Figures 5 and 6 show the relations between the quadrupole splitting and the quadratic elongation and the variance of bond angles for chain silicates, respectively. Robinson et al. (1971) demonstrated that the quadratic elongation and the variance of bond angles are linearly correlated to each other, hence Figures 5 and 6 are similar to one another. Quadrupole splitting increases very rapidly when the quadratic elongation and the variance of the bond angles are in the range of $\langle\lambda\rangle$ = 1.0060–1.0088 and σ^2 = 17.4–28.7, respectively. When $\langle\lambda\rangle$ and σ^2 equal 1.0099 and 33.68, respectively, the quadrupole splitting reaches a maximum value of Δ = 2.8 mm/s. When $\langle\lambda\rangle$ and σ^2 are larger than 1.0187 and 59.13, respectively, the quadrupole splitting decreases. When $<\lambda>$ = 1.2523 and σ^2 = 462.1, respectively, the quadrupole splitting has the minimum value of Δ = 1.67 mm/s (Li and De Grave, in preparation). This result is in agreement with the model proposed by Ingalls (1964), and therefore, $\langle\lambda\rangle$ and σ^2 can be taken as a measure of the site distortion of the polyhedra, instead of the two lowest splittings of the crystal-field levels.

The relationship between the quadrupole splitting and the quadratic elongation and the variance of bond angles have not been established for phosphate minerals, because of lack of data. However, the correlations observed for chain silicates are consistent with Ingalls's model being applied to Fe^{2+} containing compounds, and they can be consulted when assigning QSDs to Fe^{2+} in different sites in phosphates and other minerals.

The values of $\langle\lambda\rangle$ and σ^2, as well as the bond lengths for arrojadite, are given in Table 3. Compared with those sites with $\langle\lambda\rangle$ = 1.0060–1.0088 and σ^2 = 17.4–28.7 in chain silicates, the M3, M4, M5, M6, and M7 octahedral sites in arrojadite are more distorted. Therefore, it is proposed that the quadrupole splitting of Fe^{2+} in these former sites in the arrojadite decreases with increasing octahedral distortion. We have tentatively assigned QSDs with the largest quadrupole splitting Δ to Fe^{2+} in the M3 site with the smallest distortion, and QSDs with the smallest quadrupole splitting Δ to Fe^{2+} in the M5 site with the largest distortion, respectively (Table 1). The QSDs with intermediate quadrupole splittings Δ are assigned to Fe^{2+} in the M6, M7, and M4 sites, respectively, since the quadratic elongation and the variances of bond length of these sites fall between those of the M3 and M5 sites. The iron distribution over the different sites can be obtained on the basis of the Mössbauer areas listed in Table 1.

The isomer shifts for the corresponding QSDs at 95 K are 0.04–0.06 mm/s larger than those at 298 K. This is

TABLE 3. Site parameters of arrojadite

Site	d(Å)*	Coordination	σ²†	⟨λ⟩†
M1	2.022	4O		
M2	2.100	5O		
M3	2.106	5O,1F	41.92	1.015
M4	2.143	6O	114.58	1.036
M5	2.148	6O	136.73	1.042
M6	2.206	5O,1F	65.45	1.022
M7	2.148	5O		
M7‡	2.38	6O	98.85	1.034

* The average bond lengths obtained by Moore et al. (1981).
† The values of quadratic elongation ⟨λ⟩ and variance of bond angles σ^2 were calculated, based on the structural data obtained by Moore et al. (1981).
‡ Preferred arrangement.

TABLE 4. Mean isomer shifts and average bond lengths of representative phosphate and silicate minerals

Mineral class	Site	δ (mm/s)		d(Å)		δ/d	Reference
		Range	Mean	Range	Average		
Phosphates	Octahedron	1.15–1.274	1.217	2.007–2.37	2.16	0.563	This study (Table 2)
Silicates	Octahedron	1.13–1.17	1.15	2.112–2.168	2.15	0.534	Li and De Grave (1995)
Phosphates	Bipyramid	1.10–1.16	1.13	2.00–2.134	2.058	0.549	This study (Table 2)
Silicates	Bipyramid	1.10	1.10	2.04	2.04	0.539	Li and De Grave (1995)

caused by a second order Doppler effect. The quadrupole splitting for the corresponding QSDs at 95 K are 0.18–0.73 mm/s larger than those at 298 K. All Mössbauer parameters change in a similar manner with temperature, and the ratio of the absorption area at 95 K is consistent with that at 298 K.

Comparison of phosphate with silicate minerals

Li and De Grave (1995) and Li (1995) summarized isomer shift data and average bond length data for representative silicate minerals. A nearly linear correlation exists between the isomer shifts and average bond lengths. The isomer shifts of Fe^{2+} in octahedral sites with average bond lengths d = 2.112–2.168 Å are in the range of 1.13–1.17 mm/s, while the corresponding value for a distorted bipyramid with d = 2.04 Å in grandidierite is equal to 1.10 mm/s. Table 4 presents the ranges and the mean values for the isomer shift and average bond length for some representative phosphate and silicate minerals. The mean isomer shift of Fe^{2+} in octahedral sites in silicate minerals is ~0.07 mm/s less than that in phosphate minerals, although the mean bond lengths are similar. The values δ/d for phosphate minerals are 0.01–0.03 mm/s larger than those for silicate minerals. It is well known that electronegativity is the tendency of an atom to acquire a negative charge. The electron affinity has been suggested as a measure of electronegativity of a neutral atom. The greater the numerical difference between an element pair, the more ionic their bonds. Thus, Si-O bonds in silicate minerals (13.62 − 8.15 eV = 5.47 eV) are more ionic than P-O bonds (13.62 − 10.90 eV = 2.72 eV). Hence, the O atoms having a more covalent bond character in phosphate minerals are more effective in withdrawing s-electron density from the iron nucleus, resulting in higher isomer shift values.

ACKNOWLEDGMENTS

We acknowledge R. Thiel and J.Y. Ping for constructive reviews of the manuscript. We are grateful to D.N. Ye for helpful discussion. We also thank J.Y. Ping for kindly providing the computer program. This project was supported by the Japan Society for the Promotion of Science (JSPS) and the National Science Foundation of China (NSFC).

REFERENCES CITED

Burns, R.G. (1981) Intervalence transitions in mixed valence minerals of iron and titanium. Review of Earth and Planet Science, 9, 345–383.

Chandra, S. and Hoy, G.R. (1967) Detection of two internal magnetic fields in $Fe_3(PO_4)_2 4H_2O$. Physical Letters, 24A, 377–378.

Charalampides, G., Ericsson, T., Nord, A.G., and Khangi, F. (1988) Studies of hydrothermally prepared $(Fe,M)_3(PO_4)_2$-sarcopsides. Neues Jahrbuch Für Mineralogie Monatshefte, 1988, 324–336.

Dormann, J.L. and Poullen, J.F. (1980) Etude par spectroscopie Mössbauer de vivianites oxydees naturelles. Bulletin of Mineralogy, 103, 633–639.

Ericsson, T. and Nord, A.G. (1984) Strong cation ordering in olivine-related (Ni,Fe)-sarcopsides: A combined Mössbauer, X-ray and neutron diffraction study. American Mineralogist, 69, 889–895.

Ericsson, T., Nord, A.G., and Aberg, G. (1986) Cation partitioning in hydrothermally prepared olivine-related (Fe,Mn)-sarcopsides. American Mineralogist, 71, 136–141.

Gonser, U. and Grant, R.W. (1967) Determination of spin directions and electric field gradient axes in vivianite by polarized recoilfree gamma-rays. Physica Status Solidi, 21, 331–342.

Guimaraes, D.J. (1942) Arrojadite, um novo mineral do grupo da Wagnerita. Boletin Faculdad Filosofie Clencias Letters XXX (São Paulo), Mineralogia, 5, 4–15.

Headden, W.P. (1891) A phosphate near triphylite from the Black Hills. American Journal of Science, 41, 416–417.

Ingalls, R. (1964) Electric field gradient tensor in ferrous compounds. Physical Review, A133, 787–795.

Ito, T. and Mori, H. (1951) The crystal structure of ludlamite. Acta crystallographica, 4, 412–416.

Kostiner, E. (1972) A Mössbauer effect study of triplite and related minerals. American Mineralogist, 57, 1109–1114.

Li, Z. (1995) Correlation of Fe^{2+} isomer shift with average atom distance in silicate minerals. Chinese Science Bulletin, 40, 1017–1021.

Li, Z. and De Grave, E. (1995) The correlation of Fe^{2+} isomer shifts with bond lengths and bond strengths in neso- and sorosilicates. Science in China, 38, 478–483.

Lindberg, M.L. (1950) Arrojadite, huhnerkobelite, and graftonite. American Mineralogist, 35, 59–76.

Mason, B. (1941) Minerals of the Varutrask pegmatite. XXIII some iron-manganese phosphate minerals and their alteration products, with special reference to material from Varutrask. Geologiska Foreningens Forhandlingar, 63, 129–134.

Mattievich, E. and Danon, J. (1977) Hydrothermal synthesis and Mössbauer studies of ferrous phosphates of the homologous series $Fe_3^{2+}(PO_4)_2(H_2O)_n$. Journal of Inoganic and Nuclear Chemistry, 39, 569–580.

McCammon, C.A. and Burns, R.G. (1980) The oxidation mechanism of vivianite as studied by Mössbauer spectroscopy. American Mineralogist, 65, 361–366.

Moore, P.B. (1972) Sarcopside: its atomic arrangement. American Mineralogist, 57, 24–35.

Moore, P.B. and Araki, T. (1973) Hureaulite, $Mn_5^{2+}(H_2O)_4[PO_3(OH)]_2[PO_4]_2$: Its atomic arrangement. American Mineralogist, 58, 302–307.

———(1976) A mixed-valence solid solution series: crystal structure of phosphoferrite, $Fe_3^{2+}(H_2O)_3(PO_4)_2$ and kryzhanovskite, $Fe_2^{3+}(OH)_3(PO_4)_2$. Inorganic Chemistry, 15, 316–321.

Moore, P.B. and Ito, J. (1979) Alluaudites, wyllieites, arrojadites: crystal chemistry and nomenclature. Mineralogical Magazine, 43, 227–235.

Moore, P.B., Araki, T., Merlino, S., Mellini, M., and Zanazzi, P.F. (1981) The arrojadite-dickinsonite series, $KNa_4Ca(Fe,Mn)^{2+}{}_{14}Al(OH)_2(PO_4)_{12}$: crystal structure and crystal chemistry. American Mineralogist, 66, 1034–1049.

Mori, H. and Ito, T. (1950) The structure of vivianite and simplesite. Acta Crystallographica, 3, 1–6.

Nomura, K. and Ujihira, Y. (1982) Mössbauer spectroscopic study of hureaulite. Nippon Kagaku Kaishi, 1352–1356.

Nord, A.G. and Ericsson, T. (1982) The cation distribution in synthetic

$(Fe,Mn)_3(PO_4)_2$ graftonite-type solid solutions. American Mineralogist, 67, 826–832.

———(1985) Cation distribution studies of some ternary orthophosphates having the farringtonite structure. American Mineralogist, 70, 624–629.

Nord, A.G., Aberg, G., Annersten, H., Ericsson, T., and Stefanidis, T. (1985) Farringtonite-related $(Co,Fe)_3(PO_4)_2$ phases: A combined Mössbauer spectroscopy and X-ray, electron and neutron diffraction study. Chemical Scripa, 25, 189–193.

Ping, J.Y., Rancourt, D.G., and Stadnik, Z.M. (1991) Voigt-based methods for arbitrary shape quadrupole splitting distributions (QSDs) applied to quasi-crystals. Hyperfine Interactions, 69, 493–496.

Quensel, P. (1937) Minerals of the Varutrask pegmatite. I. The lithium-manganese phosphates. Geologika Foreningens Forhandlingar, 59, 77–96.

Rancourt, D.G. and Ping, J.Y. (1991a) Voigt-based method for arbitrary-shape static hyperfine parameter distributions in Mössbauer spectroscopy. Nuclear Instruments and Methods in Physics Research, B58, 85–97.

———(1991b) Measured and predicted hyperfine field distributions (HFDs) in Fe-Ni collinear ferromagnets. Hyperfine Interactions, 69, 497–500.

Rancourt, D.G. (1994a) Mössbauer spectroscopy of minerals: I. Inadequacy of Lorentzian-line doublets in fitting spectra arising from quadrupole splitting distributions. Physics and Chemistry of Minerals, 21, 244–249.

———(1994b) Mössbauer spectroscopy of minerals: II. Problem of resolving cis and trans octahedral Fe^{2+} sites. Physics and Chemistry of Minerals, 21, 250–257.

Rancourt, D.G., Ping, J.Y., and Berman, R.G. (1994) Mössbauer spectroscopy of minerals: III. Octahedral-site quadrupole splitting distributions in the phlogopite-annite series. Physics and Chemistry of Minerals, 21, 258–267.

Rancourt, D.G., Ping, J.Y., Boukili, B., and Robert, J.L. (1996) Octahedral-site Fe^{2+} quadrupole splitting distributions from Mössbauer spectroscopy along the (OH, F)-Anita join. Physics and Chemistry of Minerals, 23, 63–71.

Robinson, K., Gibbs, G.V., and Ribbe, P.H. (1971) Quadratic elongation: a quantitative measure of distortion in coordination polyhedra. Science, 172, 567–570.

Scheideler, J.A. and Terry, C. (1969) Mössbauer effect in antiferromagnetic $Li(Fe,Mn)PO_4$. Physical Letters, 28A, 759–761.

Takashima, Y. and Ohashi, S. (1968) The Mössbauer spectra of various natural minerals. Bulletin of Chemical Society of Japan, 41, 88–93.

Tricker, M.J. and Ash, L.A. (1979) On the anomalous inertness to oxidation of the surface regions of vivianite: A conversion electron and transmission Mössbauer study. Journal of Inorganic and Nuclear Chemistry, 41, 891–893.

Vochten, R., De Grave, E., and Stoops, G. (1979) Petrography, chemical and Mössbauer study of some oxidized vivianite from Retie (Province of Antwerp, Belgium). Neues Jahrbuch für Mineralogie Monatshefte, 1979, 208–222.

Waldrop, L. (1969) The crystal structure of triplite $(Mn, Fe)_2FPO_4$. Zeitschrift für Kristallographie, 130, 1–14.

———(1970) The crystal structure of triploidite and its relation to the structure of other minerals of triplite-triploidite group. Zeitschrift für Kristallographie, 131, 1–20.

Ziegler, V. (1914) The minerals of the Black Hills, South Dakota School of Mines Bulletin, 10, 192–194.

Manuscript received January 19, 1998
Manuscript accepted June 14, 1998
Paper handled by Charles A. Geiger